Chapter 1

Introduction

1.1 Background

Prior to the mid-20^{th} century, catastrophic structural failures, such as those observed in Liberty ships (Figure 1.1), often occurred unexpectedly and could not be explained within the framework of designed principles based on the assumption of flawless materials. Subsequent investigations concluded that welding defects and discontinuities (i.e., sites where cracks/notches can form) contributed to each failure.

The discipline of Fracture Mechanics (FM) received limited attention before the Second World War. Structural cracks were primarily dismissed as trivial imperfections which were unlikely to compromise the integrity of significant constructs. Cracks in major structures, whether ships, aircraft, buildings, etc., were often overlooked and viewed as minor imperfections that wouldn't impact the overall integrity of the construction. This assumption was based on the broadly accepted but flawed belief

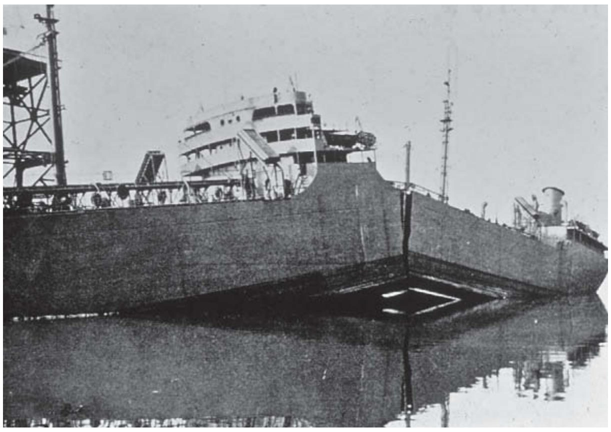

FIGURE 1.1: The Liberty ship S.S. Schenectady, which, in 1943, failed before leaving the shipyard. The incidents drew major attention to the study of cracks. Source: WordPress

that materials were inherently without defects and that their properties were uniform and isotropic [1].

The emergence of FM as an entirely separate field changed this perspective by acknowledging that defects in materials are almost inevitable, whether they arise during the manufacturing process or under the stresses of normal operations.

Another notable incident underscoring the fallacy of this assumption occurred in 1919 with the "Boston Molasses Disaster" in Boston, Massachusetts (Figure 1.2). A colossal storage tank burst, unleashing a deluge of molasses that surged through the streets at approximately 35 miles per hour. This calamity claimed 21 lives and caused injuries to 150 individuals. Subsequent engineering analyses over the ensuing century have thoroughly investigated this incident. The tank's failure was ultimately ascribed to a fatigue crack at its base, precipitated by cyclic loading due to repeated filling and emptying and substandard construction practices. Many years later, investigations indicated that the probable cause was a brittle fracture of the tank at rivets, with the temperature below the ductile to brittle transition temperature.

[1] there were no preferred directions in the material

FIGURE 1.2: The Great Boston Molasses Disaster. Twenty-one people were killed, and more than 150 buildings were destroyed as the result of 2.3 million gallons of molasses flooding North Boston. Investigations indicated the probable cause to be brittle fractures.

The exigencies experienced during World War II served as a critical juncture, shedding light on the inadequacies inherent within the prevailing assumptions about material science. It became increasingly clear that an enhanced understanding of material behaviour under various stress conditions was essential for developing more resilient materials. Failure means the inability of a material to perform the specified functions, but despite maximum efforts and material properties, it is impossible to avoid failures. Failures within materials can manifest in various forms [3], including but not limited to

(i) Elastic deformation transitioning into the plastic range,

(ii) material damage accumulation,

(iii) initiation and growth of microcracks,

(iv) propagation of cracks through the materials.

These phenomena underscore the complexity of material failure mechanisms. Fractures are several forms of failures that can persist in a structure. Notably, the formation of cracks represents a significant vulnerability, as these two-dimensional defects not only diminish the effective cross-sectional area of material but also introduce localized stress concentrations, thereby exacerbating the risk of material failure. Hence, the criticality of crack formation and its subsequent propagation in the context of solid mechanics cannot be overstated. This intense scrutiny is justified by cracks' pivotal role in compromising structural integrity. Numerous case studies and empirical analyses have unequivocally linked material failures to the emergence and expansion of cracks within structural components [10, 2]. The field of FM is concerned with characterising and analysing the mechanics of deformable bodies with cracks present in them. This analytical approach provides indispensable insights into the potential pathways through which material failure might ensue, offering a nuanced understanding of the interplay between material properties and applied stresses. Therefore, studying stress distribution near a crack tip emerges as a cornerstone of FM. This led to the emergence of new concepts in FM, viz., Stress intensity factors (SIF), fracture toughness, energy criterion, etc. Moreover, it contributes to the broader discourse on material resilience, propelling the development of materials capable of withstanding significant stress without succumbing to failure [11].

1.2 Overview

The field of fracture mechanics focuses on quantitatively describing the mechanical state of a deformed body that contains cracks. This involves creating a mathematical model and drawing conclusions using mathematical and numerical analysis. Fracture mechanics considers applied stresses, the size of the faults, and fracture toughness. The stress intensity approach is one alternative method for analyzing fractures (Figure 1.3). The fundamentals of fracture mechanics are discussed in detail in the subsequent sections and sub-sections of the chapter. A significant figure in the development of fracture mechanics was A. A. Griffith, an English aeronautical engineer

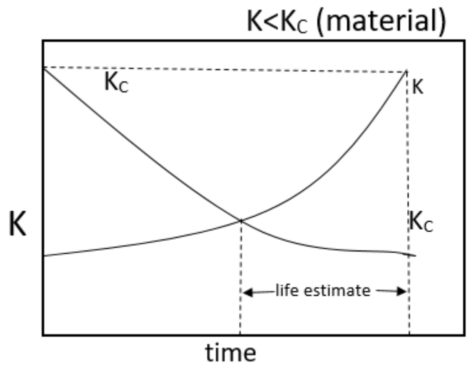

FIGURE 1.3: Diagram showing life prediction procedure and failure criteria (Fracture Mechanics Approach) [2].

who made significant advances in understanding brittle fracture mechanisms during the First World War. Griffith's brilliance stemmed from his application of analytical methods to the laws of thermodynamics and energy balance in structures containing cracks, laying the groundwork for analyzing brittle fractures in materials. Despite his groundbreaking work in understanding fracture mechanics, Griffith faced challenges in creating a universally applicable metric for predicting the load at which a component would fail due to crack propagation [12]. However, the significance of his work lies in introducing fundamental concepts such as critical stress intensity factors. His contributions gave rise to the term "Griffith crack", summarizing the essence of brittle fracture phenomena [11]. In 1913, C.E.Inglis calculated stress concentration near elliptic holes, but this solution possessed a mathematical complexity for sharp cracks, and the stresses became infinity at the tip of the sharp crack. In the decade following the war, the exploration of FM was constrained within the realms of linear elastic mechanics. This perspective dominated until the advancements in the 1960s, which marked a paradigm shift towards incorporating nonlinear mechanics and acknowledging the plasticity behaviour of metals. Thus, the landscape of FM research expanded significantly. A key moment in the history of FM was the contribution of the research group led by Dr. G. Irwin in 1948. Through his pioneering work, Irwin established practical and theoretical frameworks that significantly propelled the discipline. He introduced key parameters such as stress intensity factors and the energy release rate in 1956 [13], instrumental in advancing the field. Irwin's contributions heralded a new era, sparking a fervour of interest and research within the scientific community, thereby shaping the contemporary landscape of FM. In the wake of Irwin's influential work, notable advancements were made that further enhanced the mechanics' theoretical and practical aspects [14, 15]. The introduction of crack tip opening displacement by Wells in 1961 [16] and the conceptualization of the J-integral by Rice in 1968 [17] were significant milestones. These developments augmented the analytical toolkit available for dissecting the nuances of fracture processes, enriching the understanding of material behaviour under stress and the implications of various types of fractures [18]. These parameters will be discussed in detail later in this chapter.

1.2.1 Linear Elastic Fracture Mechanics

In FM, a significant emphasis is placed on examining material discontinuities, such as cracks, and their substantial impact on the mechanical properties of materials and their propensity to instigate failure. This discipline is multifaceted, employing various branches of FM tailored to the nuances of the problem at hand, which, in turn, are heavily influenced by the intrinsic behavioural characteristics of the material under scrutiny. Specifically, brittle fracture is identified as the predominant mode of failure in materials that exhibit low toughness. A linear relationship exists in such materials between the critical stress required to propagate a crack and the SIF. This direct correlation provides crucial insights into the fracture resistance of materials characterized by low toughness. Conversely, in the evaluation of materials exhibiting high levels of toughness, standard principles of LEFM are

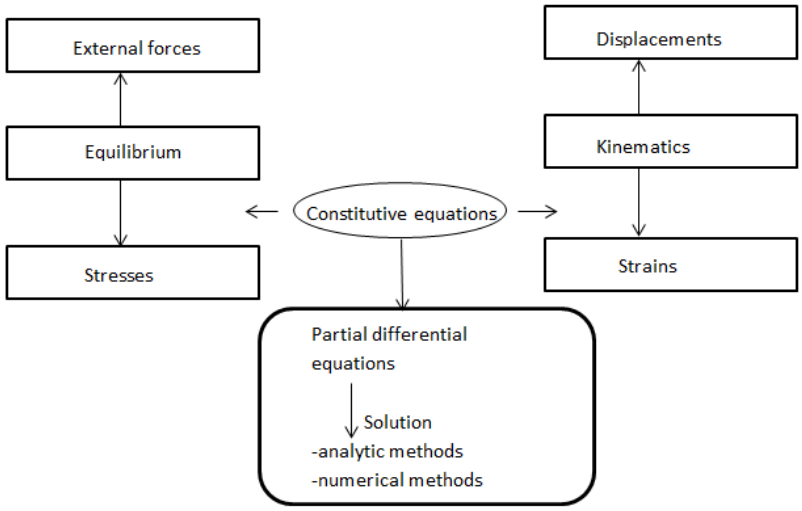

FIGURE 1.4: Diagram to depict the approach taken to tackle a problem in LEFM [3].

found to be inadequate. Instead, the failure mechanisms of such materials are predominantly governed by their flow properties. This transition highlights the need for a more comprehensive understanding of the material's flow characteristics to accurately predict failure, as extensively discussed by Anderson [4, 11]. Given the pivotal role of constitutive relations in depicting the physical behaviour of materials, especially under the influence of mechanical and thermal loadings, these relations serve as the basis for defining the mechanical response of solids (Figure 1.4). This discourse intensively delves into stress-strain constitutive relations, which form the backbone of our understanding of material response under load, detailed in the forthcoming sections of the chapter. The concentration of this discussion on simplistic elastic materials arises from the deliberate exclusion of the effects attributable to strain rate and strain history. Herein, the adoption of linear constitutive stress-strain relations is justified based on the fundamental behaviour exhibited by linear elastic materials. The rationale behind this focused discourse encompasses several facets: firstly, the abundance of literature on linear elastic materials significantly enhances the feasibility of conducting a thorough stress analysis. Secondly, the aim is to illuminate different mathematical methodologies applicable across a spectrum of loading conditions, thereby augmenting the versatility of analytical approaches for crack problems in orthotropic materials [19]. The strength of the linear elastic FM approach to assessing fracture or fatigue crack growth from crack-like defects lies in the proposition that data derived from small laboratory specimens can be used to assess the behaviour of larger structures because these physical phenomena are uniquely related to the crack tip stress intensity factor, "K".

Moreover, an extensive array of structural materials—including metals, ceramics, concrete, and wood—demonstrate predominantly linear elastic behaviour when subjected to minimal deformations. This observation anchors the rationale for focusing on elastic materials and facilitates the derivation of closed-form solutions for considered problems. Such an approach is instrumental in addressing and mitigating the complexities associated with stress singularity. Within the framework of this analytical perspective, the influence wielded by the plastic zone is negligible. This methodological simplification is advocated for based on its theoretical and computational efficiencies, thereby endorsing its viability across a broad spectrum of engineering applications [18].

The stress-strain curve for three materials is illustrated in Figure 1.5. The point where large plastic deformation begins is called the yield point. The theory assumes that yielding due to plastic deformation occurs only within a small region surrounding the crack tip, while the rest of the material remains elastic.

As mentioned already, the principles of LEFM were developed in 1957 by George Irwin. This work was based on previous investigations of Griffith [12] and Orowan (1944) [20]. Irwin demonstrated that a crack shape in a particular location with respect to the loading geometry had a stress intensity associated with it. The strength

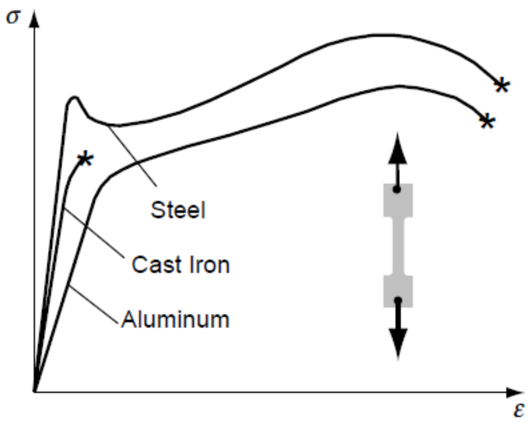

FIGURE 1.5: Stress-strain curve [3].

of any product is limited by the size of the cracks or defects during processing, production and handling. The ranch of FM one should apply depends on the material behaviours considered. For low-toughness brittle materials LEFM is adequate to analyse the governing failure mechanism.

1.2.2 Stress

Stress is the major contributing factor to material failure. In the thesis, the elasticity theory has been applied to determine the distribution of stresses within the considered plane, and the imposed condition is that the force distribution at each point within the body must be balanced. The nine stress components, written in the traction vector form as $\{\sigma_{xx},\ \sigma_{yy},\ \sigma_{zz},\ \tau_{xy},\ \tau_{yx},\ \tau_{zy},\ \tau_{yz},\ \tau_{zx},\ \tau_{xz}\}$ are the components of the second-order stress tensor σ and illustrated as in Figure 1.6. There are three normal components denoted by repeated suffixes and six shear components. Since the stress tensor is symmetric, the six independent variables are sufficient to determine the state of stress of an elastic body and are represented by the column matrix

$$\sigma = \{\sigma_{xx},\ \sigma_{yy},\ \sigma_{zz},\ \tau_{xy},\ \tau_{yz},\ \tau_{xz}\}^T, \tag{1.1}$$

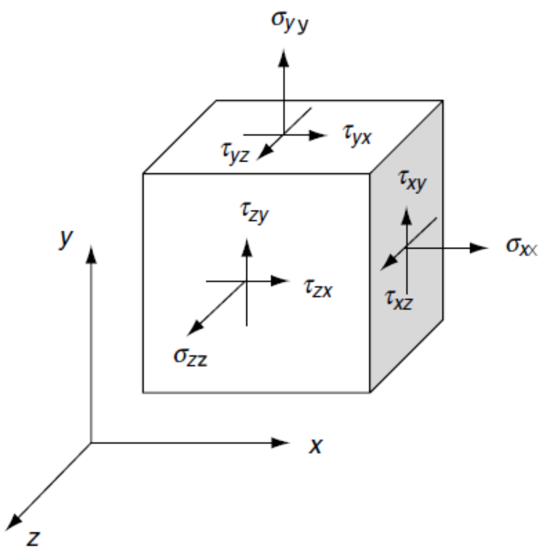

FIGURE 1.6: Stress components distribution

where the repeated subscript denotes the normal stresses and different subscript notations under τ denote shear stresses. Shear stress notation includes the plane of action and the secondary direction of the stress. The stress is defined as the stress per unit area and the S.I. unit is N/m^2.

1.2.3 Strain

A linear elastic material can have at most 21 independent elastic constants. Due to material symmetry, this number is reduced. When a 2-D deformation is considered, this number is further reduced. The important condition imposed on the 6x6 matrix is that it should be positive definite[2] This condition arises due to the fact that strain

[2]A real symmetric matrix is positive definite if $u^T cu > 0$ for any non-zero vector u.

energy must be positive [21]. The strain tensor is given in matrix format as

$$\boldsymbol{\epsilon} = \begin{bmatrix} \epsilon_{xx} & \epsilon_{xy} & \epsilon_{xz} \\ \epsilon_{xy} & \epsilon_{yy} & \epsilon_{yz} \\ \epsilon_{xz} & \epsilon_{yz} & \epsilon_{zz} \end{bmatrix}. \tag{1.2}$$

In the fixed rectangular coordinate system, the stress-strain relationship given by the generalised Hooke's law (proposed by R. Hooke in 1676) is defined as

$$\sigma_{ij} = c_{ijkl}\epsilon_{kl}, \tag{1.3}$$

where $c_{ijkl},\ i, j, k, l = 1, 2, 3$ are elastic stiffnesses and components of fourth rank tensor. They satisfy the symmetry condition

$$c_{ijlk} = c_{jikl} = c_{klij}.$$

It has already been discussed that there are 21 independent components of stiffness matrix for generalised anisotropic material, which are reduced to 13 independent components when there is one plane of symmetry and only 9 components where there are three planes of symmetry, i.e. orthotropic materials [3]. For orthotropic

[3] Materials whose mechanical properties are dependent on the orientation of the specimen are called anisotropic materials. An anisotropic material is orthotropic when it shows properties that differ along three mutually-orthogonal axes. Orthotropic materials have three mutually perpendicular orthogonal planes, for example wood

materials, the elastic tensor takes the form

$$\begin{bmatrix} C_{11} & C_{12} & C_{13} & 0 & 0 & 0 \\ C_{12} & C_{22} & C_{23} & 0 & 0 & 0 \\ C_{13} & C_{23} & C_{33} & 0 & 0 & 0 \\ 0 & 0 & 0 & C_{44} & 0 & 0 \\ 0 & 0 & 0 & 0 & C_{55} & 0 \\ 0 & 0 & 0 & 0 & 0 & C_{66} \end{bmatrix}. \tag{1.4}$$

The stiffness coefficients can be written as function of material elastic constants i.e. Young's modulus, E, Poisson ratio, ν and shear modulus, G. The isotropic materials have only two independent constants E and ν [22]. In two dimensional plane, the generalised anisotropic materials are characterized by 9 independent elastic constants and orthotropic materials have 6 independent elastic constants.

1.2.4 Stress Intensity Factor

The vicinity of the crack tip offers interesting information as the magnitudes of the stress components are extremely high. Hence, the knowledge of stress or strains near the crack tips is very useful. One of the parameters used to characterise a crack is SIF. In LEFM, the elastic analysis has been carried out in the thesis to determine crack displacements and stress fields. The parameters on which these stress fields depend are the external loads, the crack length and the geometry of the problem. The credit for defining the parameter SIF goes to Irwin, who used the symbol K after his collaborator Kies. According to the theory of linear elasticity, the components of near-tip stresses are expressed as

$$\sigma_{ij}(r,\theta) = \frac{K}{\sqrt{2\pi r}} F_{ij}(\theta), \quad \text{as } r \to 0, \tag{1.5}$$

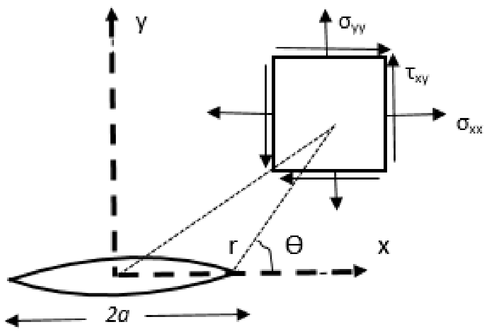

FIGURE 1.7: Coordinate axis diagram for a crack of length $2a$ [4].

where $r = 0$ coincides with the crack edge and the line $\theta = 0$ is tangent to the crack surface in the direction ahead of the crack, the function $F_{ij}(\theta)$ represents the angular variation of each crack tip stress component and the suffixes denote the various stress components. Thus, stress at the vicinity of the crack tip varies with $r^{-1/2}$ singularity. The SIF for a crack of length $2a$, as shown in Figure 1.7, is given by

$$K = \sigma \sqrt{\pi a}. \tag{1.6}$$

The critical SIF (K_c) is the limiting value of stress, after which the cracks start propagating rapidly (Figure 1.3). The S.I. unit of SIF is MPa.m$^{1/2}$.

1.2.5 Modes of fracture

The basis of classification into different modes of fracture is the contribution of components of relative displacements of particles on opposite faces of crack-to-crack face separation [5].

- Mode-I: The in-plane opening mode of crack deformation due to normal deformation of crack faces. In terms of SIF K_I for mode I, the stress and displacement components are written as

$$F_{xx}(\theta) = \cos(\theta/2)\{1 - \sin(3\theta/2)\sin(\theta/2)\}, \tag{1.7}$$

$$F_{xy}(\theta) = \cos(\theta/2)\cos(3\theta/2)\sin(\theta/2)\}, \tag{1.8}$$

$$F_{yy}(\theta) = \cos(\theta/2)\{1 + \sin(3\theta/2)\sin(\theta/2)\}. \tag{1.9}$$

- Mode-II: The in-plane shearing mode due to sliding of the crack faces in the direction perpendicular to the crack edges. In terms of SIF K_{II} for mode II, the stress and displacement components are written as

$$F_{xx}(\theta) = -\sin(\theta/2)\{2 + \cos(3\theta/2)\cos(\theta/2)\}, \tag{1.10}$$

$$F_{xy}(\theta) = \cos(\theta/2)\{1 - \sin(3\theta/2)\sin(\theta/2)\}, \tag{1.11}$$

$$F_{yy}(\theta) = \cos(\theta/2)\cos(3\theta/2)\sin(\theta/2)\}. \tag{1.12}$$

- Mode-III: The antiplane out-of-plane shearing mode due to sliding of crack faces in the direction tangent to crack edges. In terms of SIF K_{III} for mode III, the stress and displacement components are written as

$$F_{zx}(\theta) = -\sin(\theta/2), \tag{1.13}$$

$$F_{zy}(\theta) = \cos(\theta/2). \tag{1.14}$$

The classification is depicted in Figure 1.8 where the direction of crack opening displacement is also indicated.

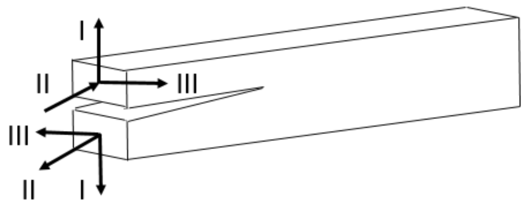

FIGURE 1.8: Different modes of fracture based on the stress component acting on the crack surface [5].

1.2.6 Crack Opening Displacements (COD)

The crack displacement components are finite quantities and are free of any singularities. The distance between two crack faces is known as COD and is a useful parameter for carrying out experiments and determining the crack tip opening displacements. In the thesis, the terms crack opening displacement and crack sling displacement have been used to denote different displacements.

1.2.7 Heat Flux Intensity Factor (HFIF)

HFIF is a parameter used to define the singularity of heat flux near the crack tip. The heat flux and temperature gradients near the tip of a crack exhibit the $r^{-1/2}$ singularity, which affects the behaviour of crack propagation and failure in structures under thermo-mechanical loading [23]. In the groundbreaking study by Sih [24], it was found that heat fluxes possess the characteristic inverse square-root singularity in terms of the radial distance from the point of the line of discontinuity, reaching mathematically infinite values at the point itself. According to the study of Sih, the local heat fluxes are expressed as

$$q_x = -\frac{K_H}{\sqrt{r}} \sin(\theta/2) + O(r^{1/2}), \tag{1.15}$$

$$q_y = -\frac{K_H}{\sqrt{r}} \cos(\theta/2) + O(r^{1/2}). \tag{1.16}$$

Due to this singular behaviour, the HFIF is introduced to quantify the thermal energy accumulated near the crack tip [25]. In the presence of uniform heat flow q_o, the HFIF is defined as

$$K_H = \lim_{r \to 0} \sqrt{2\ r}\ q_o, \tag{1.17}$$

the factor $K_H = K_H(q_o, a, \theta)$ depends on the loadings, problem geometry, and crack orientation. The HFIF describes the strength of singularity at the crack tip and is important for understanding the thermal behaviour of high-temperature materials and structures.

1.3 Literature survey

FM employs a variety of techniques and methodologies to calculate SIFs under diverse loading scenarios. Many research articles have addressed the problems of interfacial cracks in anisotropic medium. The SIF at the crack tip is a parameter introduced by G.R. Irwin in 1957 that could yield information about load, composite geometry, and material that would affect the local stress field. The SIF is useful to study the fracture behaviour of layered composites. The stress field contains squared root singularity at the interface crack tip [26, 27]. The principle mechanism of fracture failures in composite materials is explained in detail in many monographs and books such as Altenbach [28], Anderson [11], Kumar [18], Ochsner [3]. Presently, the significance and practical application of these principles in engineering mechanics are paralleled only by the mechanics of composites. This opinion is supported by the fact that two eight-volume collective fundamental monographs of encyclopedic nature were published in the middle of the second half of the *20th* century. The first one, monograph [29], deals with problems of composite materials, including the mechanics of composites, while the second one, monograph [30], considers the problems of materials destruction, including fracture mechanics. Milton [31] presents an introduction to the theory of composite materials, encompassing the electrical, thermal, magnetic, thermoelectric, mechanical, piezoelectric, poroelastic, and electromagnetic properties. Due to the complicated properties of orthotropic materials, their fracture analysis is of great importance due to inherent flaws like debonded interfaces, voids, etc., from an application point of view. Different approaches, viz., the stress and energy approaches, are used to study fracture mechanics problems. The stress-based criteria, which have been utilised in the thesis, are appropriate for the problems with fracture onset. In this thesis, the theoretical study of mode I/II fracture criteria for the assessment of composite materials has been considered. Problems with out-of-plane shear components have also been discussed. Sadd has defined the concepts and theory of elasticity in his book, which have been used throughout the thesis [21]. The critical insights into the stress fields at the tip of elliptical formations were significantly expanded upon by Inglis, who underscored the pronounced impact of material discontinuities, including the presence of minute cracks, on the escalation of local stress levels. Inglis's formulation for computing the stress in the vicinity of elliptical cracks has been a cornerstone in the field [27]. Furthermore, the pioneering work by Griffith introduced a novel perspective by integrating the energy balance concept in the analysis of cracked plates, thereby determining the requisite energy for the propagation of cracks. Although Griffith's theory was primarily validated for materials with homogeneous and brittle characteristics, such as glass, it laid a robust foundation for the development of FM [12]. The theoretical underpinning of FM has been significantly strengthened through the contributions of eminent scholars such as Willis (1967), Eshelby (1969), Kostrov (1974), and Freund (1990). Their work has not only provided a deep mathematical framework but also broadened the applicability of FM across a diverse array of materials, encompassing both non-isotropic and non-homogeneous types [32, 33, 34, 35]. This expansion of FM's theoretical base has enabled a more comprehensive understanding of material behaviour under stress, facilitating advancements in material design, safety assessments, and the development of novel materials with enhanced performance characteristics. The collective efforts of these researchers have thus paved the way for significant advancements in the field of materials science, enabling a sophisticated analysis of stresses that cater to a wide range of materials and applications. The ongoing evolution of FM, fueled by these foundational studies, continues to be a critical area of research, with potential implications across various sectors, including aerospace, automotive, civil engineering, and beyond, where the integrity and performance of materials under stress are of paramount importance. Based on the theory of thermoelasticity, many efforts have been made to analyse a cracked solid thermoelastic. Itou (2001) [36] has examined the thermally insulated surface with two parallel cracks by calculating SIF numerically for steel and ceramic-fiber-reinforced ceramics. Zhong et al. (2013) proposed a thermal-medium crack model to address the effects of the medium inside cracks where the boundary-valve problem is reduced to solving triple integral equations, then to solving singular integral equations with the Cauchy kernel [37]. Thangjitham et. al. [38] studied the steady-state thermoelasticity problem of a cracked fibre-reinforced slab under a state of generalized plane deformation.

1.4 Objectives

The aims of the present research works are as follows.

- To develop research for multiple cracks in a plane with specifications such as linear elastic, orthotropic, and homogenous medium with isothermal and non-isothermal conditions.

- Analytical determination of physical parameters is necessary for characterising fracture toughness like stress intensity factors of different modes of cracks, energy release rates, crack opening displacements in case of mode I crack and crack sliding displacement in mode II cracks.

- To verify and compare the results obtained with the previous results for the methods applied.

- To use analytical and numerical methods to solve the problems of multiple cracks in brittle materials viz., collocation method, Schmidt method, Wiener-Hopf method.

- To provide a detailed analysis of how the cracks interact with each other under certain thermal conditions and traction conditions.

1.5 Procedure

In the chapters of the thesis, embedded as well as interface cracks have been considered in different orthotropic composite media. Some of the considered materials are Epoxy, Aluminium, Graphite Epoxy, and Tyrannohex. To apply the mathematical methods to the considered problems, it is customary to define the geometric configuration of the body under consideration, establish relationships between stresses and cracked body, and pertinent the equilibrium laws [5]. In the subsequent chapters of the thesis, one can find the problem formulation and methodology applied sections, which contain the details of the corresponding problems.

(i) For the thermal and mechanical components, the first step is the formulation of the problem and the mathematical model by partial differential equations and appropriate boundary and continuity conditions. Defining the two-dimensional vector $\boldsymbol{x} = (x, y)$ and strain fields as $\boldsymbol{\epsilon(x)}$, the kinematic equation relates displacements to the small strains as

$$\epsilon_{ij} = \frac{1}{2}\Big(u_{i,j} + u_{j,i}\Big). \tag{1.18}$$

These strain components are directly related to the displacement functions $u(x, y)$, $v(x, y)$ and hence are not arbitrarily chosen. In the two-dimensional case, only three strain components are necessary [4].

$$\epsilon_{xx} = u_{,x}, \tag{1.19}$$

$$\epsilon_{yy} = v_{,y}, \tag{1.20}$$

$$\epsilon_{xy} = \frac{1}{2}\left(u_{,y} + v_{,x}\right). \tag{1.21}$$

The constitutive equations related to stress and strain are defined in equation (1.3). For the elastic linear isotropic medium, the stress-strain relationships are known as

$$\epsilon_{xx} = \frac{1}{E}(\sigma_{xx} - \nu\sigma_{yy}), \tag{1.22}$$

$$\epsilon_{yy} = \frac{1}{E}(\sigma_{yy} - \nu\sigma_{xx}), \tag{1.23}$$

$$\epsilon_{xy} = \frac{\tau_{xy}}{2\mu}, \tag{1.24}$$

where E is the Young's Modulus, μ is the shear modulus and ν is Poisson's Ratio [18, 19]. The equilibrium equation relates the external forces to the

[4] two normal strain components and one shear strain component are required to define the small deformation theory in (x,y) coordinate system.

internal reactions and measures the materials' loading.

$$\frac{\partial \sigma_{ij}}{\partial x_j} + \rho f_i = \rho \frac{\partial u_i}{\partial t}, \tag{1.25}$$

where $f_i(x,t)$ is body force, $\rho(x,t)$ is mass density of material at the time t. The problem is FM, in the absence of anybody forces[5] exhibit the following equilibrium equations

$$\sigma_{xx,x} + \tau_{xy,y} = 0, \tag{1.26}$$

$$\sigma_{xx,y} + \tau_{xy,x} = 0. \tag{1.27}$$

Combination of the three equations of equilibrium, kinematics and constitutive relation results in a partial differential equation, describes the entire problem. The complexities of the microscopic level are avoided by considering the equations of classical mechanics at the macroscopic level for the orthotropic materials. Compatibility condition: Keeping the strain-displacement relationship given in equations (1.19), when the displacements are continuous, single-valued and integrable, they give rise to well-behaved strains, but the reverse does not hold, i.e., integration of strain-components does not necessarily gives single-valued displacement functions [21]. This gives rise to the compatibility condition.

(ii) Next, the boundary conditions must satisfy the above equations at each point of the plane and are specified on the boundary of the body such that

- the traction is specified,

[5] Forces that act throughout the volume of the body, e.g. electric field, magnetic field, force due to gravity, etc.

- the displacements are specified.

  Within the context of the problems considered in this thesis solutions are sought that satisfy both the equilibrium conditions (as expressed in the equations (1.26)) and the boundary conditions imposed on the system.

(iii) Drive is given for finding the analytical solutions of partial differential equations for the thermal component and then obtaining the solution of the thermal stress or strain components by displacements. For some geometries, analytical solutions can be obtained which offer an exact depiction of the problem under the given assumptions and specifications. In other cases, approximate solutions by using numerical techniques are required.

For the first two steps, the involved processes and the method of approaching the problem are well-defined and well-known in the literature; one come across many computational and analytical difficulties in the process, mainly due to the involvement of multiple physical parameters. The application of the methods includes determining SIFs under certain surface forces, COD, crack interaction, etc.

1.6 Preliminaries

This section contains the definitions, formulae and relevant relations that are followed by the standard mathematical concepts used in the thesis.

1.6.1 Fourier Integral Transform

The Fourier transform is a generalization of the complex Fourier series in the limit as $l \to \infty$. The discrete coefficients are replaced with the continuous $F(x)$. Then, change the sum to an integral, and the equations become

$$f(x) = \int_{-\infty}^{\infty} F(k) e^{2\pi \iota x s} \, ds,$$

$$F(s) = \int_{-\infty}^{\infty} f(x) e^{-2\pi \iota s x} \, dx.$$

The Fourier integral is useful to analyse non-periodic functions of variable x in the range $(-\infty, \infty)$ as a linear combination of exponential functions. Such an analysis is useful because it effectively treats linear partial differential equations with coefficients independent of x subject to boundary conditions given on x, which varied from $-\infty$ to ∞ independently of other variables. To apply these boundary conditions, it is necessary to be able to write any functions occurring in them in terms of the Fourier integral. In the thesis, the semi-infinite Fourier integrals have also been used in the range $(0, \infty)$. For example, in order to determine a function $u(x)$ in this range, it can be considered an odd function in the full range $(-\infty, \infty)$ which coincides with $u(x)$ in $(0, \infty)$ [39]. Then, the Fourier transform can be written as

$$g(s) = \int_{0}^{\infty} u(x) \sin(sx) dx,$$

which is also an odd function, so that the expression of $u(x)$ in terms of $g(s)$ becomes

$$u(x) = \int_{0}^{\infty} g(s) \sin(sx) ds.$$

The above integrals are Fourier sine integrals.

Suppose $f(x)$ is a function defined over the interval $(-\infty, \infty)$ such that it satisfies the following conditions

(I) absolutely integrable over the defined interval,

(II) has a finite number of maxima and minima in every finite interval, and

(III) has a finite number of discontinuities in every finite interval, and each of the discontinuities is finite.

Hence, the Fourier cosine and sine transformations on arbitrary functions $f(x)$ and $g(x)$ are expressed as

$$\hat{f}(s) = \sqrt{\frac{2}{\pi}} \int_0^\infty f(x) \cos(sx) dx, \tag{1.28a}$$

$$\overline{g}(s) = \sqrt{\frac{2}{\pi}} \int_0^\infty g(x) \sin(sx) dx. \tag{1.28b}$$

1.6.2 Inverse Fourier Transform

Corresponding to the definitions of Fourier internal transforms defined in sub-section 1.6.1, the Inverse Fourier transforms are defined as

$$f(x) = \int_0^\infty \hat{f}(s) \cos(sx) ds, \tag{1.29a}$$

$$g(x) = \int_0^\infty \overline{g}(s) \sin(sx) ds. \tag{1.29b}$$

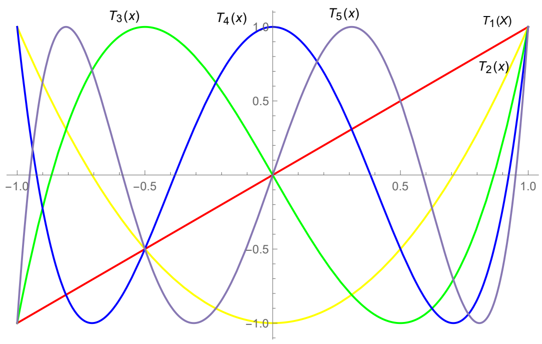

FIGURE 1.9: Chebyshev Polynomials of the first kind for different values of n.

1.6.3 Chebyshev Polynomial of the First kind

The Chebyshev polynomials of the first kind are a set of orthogonal polynomials defined as the solutions to the Chebyshev differential equation given by

$$(1-x^2)\,\frac{d^2y}{dx^2}-x\frac{dy}{dx}+\alpha^2y=0,\ |x|<1,$$

and is denoted $T_n(x)$. These are used as an approximation to the least squared fit and are a special case of the Gegenbauer polynomial with $\alpha = 0$. Those are also intimately connected with trigonometric multiple-angle formulas. The Chebyshev polynomials of the first kind, $T_i(x)$ is defined by

$$T_n(x)=\cos\left(\mathrm{n}\cos^{-1}(x)\right),$$

or

$$T_n(x)=\cosh\left(\mathrm{n}\cosh^{-1}(x)\right),$$

and satisfies the recurrence relations

$$T_o(x)=1,\ T_1(x)=x,\ T_n(x)=2x,\ T_{n-1}(x)-T_{n-2}(x),\ n\geq 2.$$

The corresponding weight function for Chebyshev polynomials of the first kind is

$$w(x) = \frac{1}{\sqrt{1-x^2}},$$

and satisfies the orthogonality condition

$$\int_{-1}^{1} \frac{T_n(x)T_m(x)}{\sqrt{1-x^2}}dx = \begin{cases} 0, & n \neq m, \\ \pi/2, & n = m \neq 0, \\ \pi, & n = m = 0. \end{cases} \tag{1.30}$$

Some of the Chebyshev polynomials are given below and graphically plotted in Figure 1.9.

$$T_o(x) = 1,$$

$$T_1(x) = x,$$

$$T_2(x) = 2x^2 - 1,$$

$$T_3(x) = 4x^3 - 3x.$$

1.6.4 Jacobi Polynomials

Jacobi polynomials are the solution of differential equation

$$(1-x^2)\,\frac{d^2y}{dx^2} - (\alpha - \beta + (\beta - \alpha + 2)x)\frac{dy}{dx} + n(n + \alpha + \beta + 1)y = 0,\ |x| < 1. \tag{1.31}$$

Jacobi polynomials are the family of orthogonal polynomials with respect to weight functions $(1-x)^{\alpha}(1-x)^{\beta}$ on the interval $[-1, 1]$. Jacobi polynomial of degree n is denoted by $P_n^{(\alpha,\beta)}(x)$. Based on the values of α and β, they are the generalisation of orthogonal polynomials like Chebyshev polynomials of the first and second kind, Legendre polynomials.

$$P_n^{(\alpha,\beta)}(x) = \frac{1}{2n}\sum_{m=0}^{n}\binom{n+\alpha}{m}\binom{n+\beta}{n-m}(x-1)^{n-m}(1+x)^m. \tag{1.32}$$

1.6.5 Bessel Function

Bessel functions of the first kind denoted by $J_n(x)$ are defined as the solutions of the Bessel differential equation as

$$x^2\,\frac{d^2y}{dx^2} + x\frac{dy}{dx} + (x^2 - n^2)y = 0, \tag{1.33}$$

which is non-singular at the origin. Some commonly used identities involving Bessel functions are [40]

$$\int_0^\infty J_n(sa)\ \cos(bs)ds = \begin{cases} \frac{\cos[n\sin^{-1}(b/a)]}{\sqrt{a^2-b^2}} & \text{if } a > b, \\ -\frac{a^n \sin[n\pi/2]}{\sqrt{b^2-a^2}[b+\sqrt{b^2-a^2}]^n} & \text{if } a < b, \end{cases} \tag{1.34}$$

$$\int_0^\infty J_n(sa)\ \sin(bs)ds = \begin{cases} \frac{\sin[n\sin^{-1}(b/a)]}{\sqrt{a^2-b^2}} & \text{if } a > b, \\ \frac{a^n \cos[n\pi/2]}{\sqrt{b^2-a^2}[b+\sqrt{b^2-a^2}]^n} & \text{if } a < b. \end{cases} \tag{1.35}$$

1.6.6 Integral Equations

An integral equation is an equation in which an unknown function appears under one or more integral signs. The general form is

$$f(x) = g(x) + \lambda\int_\Omega K(x,t)f(t)\ dt, \tag{1.36}$$

where $f(x)$ represents the unknown function, $K(x,t)$ is the kernel function, $g(t)$ is the known function, λ is arbitrary constant. The integral is taken over the interval $[a,b]$.

1.6.6.1 Classification of Integral Equations

Integral equations are classified based on different categories viz.,

- **Linear:** In an integral equation, if only linear operations are performed upon the unknown function, $f(t)$ is a linear integral equation.
- **Nonlinear**: An integral equation which is not linear is called a non-linear integral equation. For example

$$f(x) = \int_a^b K(x,t,f(t))\ dt,$$

$$\phi(x) = \lambda \int_\Omega K(x,s)\ f(s,\phi(s))\ ds, \quad x \in \Omega.$$

- **Homogeneous:** If $g(x) = 0$ in equation (1.36), it is a homogeneous integral equation. Otherwise, it is a non-homogeneous integral equation.
- **Fredholm integral equation:** FIE involves integration over the whole domain, not just up to x. FIE can be of two forms. FIE of the first kind is

$$\int_a^b K(x,t)f(t)\ dt = g(x), \tag{1.37}$$

and FIE of the second kind is

$$\lambda \int_a^b K(x,t)f(t)\ dt + f(x) = g(x). \tag{1.38}$$

Another type of integral equation is Volterra integral equation, investigated first by Vito Volterra, in which the kernel satisfies the condition [39]

$$K(x,t) = 0, \text{ if } t > x.$$

Applications [39]: Integral equations find applications in physics, engineering, and other fields. Examples include solving boundary value problems, electromagnetic theory (related to Maxwell's equations), and signal processing. Remember that integral equations provide a powerful framework for modelling various phenomena, and their study involves both theoretical analysis and numerical techniques.

1.6.7 Singular Integral Equations

A singular integral equation contains the unknown function under the integral sign of an improper integral. Specifically, it arises when the kernel function becomes unbounded (infinite) on at least one point in the interval or domain over which it is being integrated. If the kernel has singularities, it is called a singular integral equation; otherwise, it is a regular integral equation [41]. For example

$$\int_0^{\infty} \sin(tx)\ f(t)\ dt = g(x), \tag{1.39}$$

$$\int_0^{x} \frac{1}{\sqrt{x-t}}\ y(t)\ dt = f(x), \tag{1.40}$$

are some examples of singular integral equations of the first kind. One specific type of singularity addressed in the thesis is Cauchy-type singular integral equations. A FIE with a kernel of type $K(x,t) = \frac{1}{x-t}$ (equation (1.36)) is called Cauchy-type singular integral equation.

1.7 Methodology

This section provides a detailed explanation of the different mathematical methods that have been employed in the chapters of the thesis to obtain the solutions of the equations with unknown coefficients. By converting the problems of thermal and mechanical stresses, semi-analytical findings are solved using numerical computations. The mathematical backgrounds and the procedure of the numerical methods are provided here.

1.7.1 An Expansion–Collocation Approach to the Numerical Solution of Singular Integral Equations

The general form of the Cauchy-type singular integral equation of the first kind is given by

$$\int_{-1}^{1} \frac{K_o(x,r)\ f(r)}{r-x}\ \mathrm{d}r + \int_{-1}^{1} K_1(x,r)\ f(r)\ \mathrm{d}r = g(x), \quad -1 < x < 1, \tag{1.41}$$

where $K_o(x,r)$, $K_1(x,r)$ and $f(x)$ are given real-valued functions belonging to the Hölder class of continuous functions, and $f(r)$ is to be determined, occur in a variety of mixed boundary value problems in FM satisfying $K_o(r,r) \neq 0$. Assuming that the solution is unbounded at both ends of x, the unknown function f can be approximated by the polynomial function. To obtain unique solution, impose the condition

$$\int_{-1}^{1} f(x)\ dx = 0,$$

on the unknown function.

The step-by-step procedure for applying the collocation method is

- The Chebyshev polynomials of the first kind denoted by $T_n(x)$ corresponding to the weight function $W^{(j)}(x)$, has been used to approximate the auxiliary function.

- The collocation points are chosen as the zeros of the Chebyshev polynomial of degree n.

- The system of singular integral equations obtained by substituting the Chebyshev polynomials with corresponding weight functions has been computed analytically by converting them into a system of algebraic equations.

- MATHEMATICA version 12.0 is used to develop the code for the numerical results.

1.7.1.1 Chebyshev Polynomials [1]

The following integral identities are useful for numerical computations

$$\int_{-1}^{1} \frac{T_n(x)}{\sqrt{1-x^2}(x-r)} dx = \pi U_{n-1}(r). \tag{1.42}$$

Here, U_n is the Chebyshev Polynomial of the second kind.

1.7.1.2 Collocation points and approximate solution

Let the unknown function $f(x)$ in equation (1.41) be approximated by the polynomial function f_n as

$$f_n(x) = w(x) \sum_{n=0}^{n} a_n T_n(x), \tag{1.43}$$

where a_ns', are unknown coefficients. Substituting the approximate solution (1.43) for the unknown function into equation (1.41) yields

$$\sum_{n=0}^{\infty} a_n \int_{-1}^{1} \frac{w(r)T_n(r)}{r-x}\,\mathrm{d}r = g(x), \quad -1 < x < 1. \tag{1.44}$$

With some mathematical adjustments, one can rewrite this equation as

$$\sum_{n=0}^{\infty} a_n \gamma_n(x) = g(x), \quad -1 < x < 1. \tag{1.45}$$

By applying the zeroes of T_n as collocation points, let

$$x_k = \cos\left(\frac{(2k-1)\pi}{2(n+2)}\right).$$

Substituting the collocation points into equation (1.45) and using integral identities given in equations (1.30) and (1.42), the following systems of linear equations is obtained

$$\pi \sum_{n=0}^{\infty} a_n U_{n-1}\left(x_k\right) \gamma_n(x_k) = f\left(x_k\right), \quad k = 1, 2, \ldots, n. \tag{1.46}$$

1.7.2 Schmidt method

The integral equations are converted into the form of algebraic equations with unknown coefficients by making use of the complete orthogonal polynomials. Schmidt method has been utilised for numerical computations due to the complexity of the involved terms. For a given set of equations,

$$\sum_{n=1}^{\infty} b_n E_{1n} + \sum_{n=1}^{\infty} c_n E_{2n} = U_1(x),\ x \in \tau_1, \tag{1.47a}$$

$$\sum_{n=1}^{\infty} b_n E_{3n} + \sum_{n=1}^{\infty} c_n E_{4n} = U_2(x), \ x \in \tau_2. \tag{1.47b}$$

the Schmidt method is explained. The equations (1.47) are solved for coefficients b_n, c_n by using the Schmidt method [42]. A detailed explanation of the Schmidt method is given below, motivated by [43].

Weight function, $w(x)$, is a real-valued function of real variable x where

$$\int_a^b w(x)\ dx > 0.$$

Let $p_n(x)$ be polynomials of degree n with respect to positive coefficient and if $p_n(x)$ are orthonormal i.e.,

$$\int_a^b p_n(x)\ p_m(x)\ w(x)\ dx = \begin{cases} 0; & n \neq m, \\ 1; & n = m, \end{cases} \tag{1.48}$$

then $p_n(x)$ constitute system of orthogonal polynomials in interval (a, b) with respect to $w(x)$.

1.7.2.1 Procedure

A set of functions $S_n(x)$ satisfying the orthogonality condition given by

$$\int_{\tau_2} S_n(x) S_m(x) dx = N_n \delta_{nm}, \tag{1.49}$$

$$\text{where } N_m = \int_{\tau_2} S_n^2(x) dx, \tag{1.50}$$

and δ_{nm} is Kronecker delta function.

Also,

$$S_n(x) = \sum_{i=1}^{n} \frac{M_{in}}{M_{nn}} E_{4i}(x), \tag{1.51}$$

where M_{ij} is the co-factor of element d_{ij} in the matrix

$$D = \begin{bmatrix} d_{11} & d_{12} & d_{13} & .. & d_{1n} \\ d_{21} & d_{22} & d_{23} & .. & \\ d_{31} & d_{32} & d_{33} & .. & \\ .. & & & & \\ .. & & & & \\ d_{n1} & d_{n2} & d_{n3} & .. & d_{nn} \end{bmatrix}, \tag{1.52}$$

where $\quad d_{ij} = \int_{\tau_2} E_{4i}(x)\ E_{4j}(x)\ dx.$

Rewriting equation (1.47b) in terms of $S_n(x)$, we obtain

$$-\sum_{n=1}^{\infty} b_n E_{3n} + U_2(x) = \sum_{n=1}^{\infty} c_n E_{4n} = \sum_{n=1}^{\infty} a_n S_n(x), \tag{1.53}$$

where

$$a_n = \sum_{n=1}^{\infty} \alpha_{ni} c_i\ ,\ \ \alpha_{ni} = -\frac{1}{N_n} \int_{\tau_2} S_n(x) \big(E_{3n}(x) - U_2(x)\big) dx. \tag{1.54}$$

This implies

$$c_n = \sum_{n=1}^{\infty} \gamma_{ni} b_i + \delta_n, \tag{1.55}$$

$$\gamma_{ni} = -\sum_{j=n}^{\infty} \frac{M_{nj}}{M_{jj} N_j} \int_{\tau_2} E_{3i}(x)\ S_j(x)\ dx\ , \tag{1.56}$$

$$\delta_n = \sum_{j=n}^{\infty} \frac{M_{nj}}{M_{jj} N_j} \int_{\tau_2} U_2(x)\ S_j(x)\ dx. \tag{1.57}$$

Proceeding in a similar way, putting c_n in equation (1.47a),

$$\sum_{n=1}^{\infty} b_n Y_n(x) = U_1(x) - \sum_{n=1}^{\infty} \delta_n E_{2n}(x), \tag{1.58}$$

$$Y_n(x) = E_{1n}(x) + \sum_{i=1}^{\infty} \gamma_{ni} E_{2i}(x). \tag{1.59}$$

Let us define

$$\int_{\tau_1} Q_m(x)\ Q_n(x)\ dx = k_n\ \delta_{nm}, \tag{1.60}$$

where

$$k_n = \int_b^c Q_n^2(x)\ dx,$$

$$Q_m(x) = \sum_{n=1}^{n} \frac{L_{in}}{L_{nn}}\ Y_i(x), \tag{1.61}$$

where L_{ij}'s are co-factors of element e_{ij}'s of the matrix

$$E = \begin{bmatrix} e_{11} & e_{12} & e_{13} & .. & e_{1n} \\ e_{21} & e_{22} & e_{23} & .. & \\ e_{31} & e_{32} & e_{33} & .. & \\ .. & & & & \\ .. & & & & \\ e_{n1} & e_{n2} & e_{n3} & .. & e_{nn} \end{bmatrix}, \tag{1.62}$$

and

$$e_{ij} = \int_{\tau_1} Y_i(x) Y_j(x) dx.$$

Using equations (1.58) and (1.61),

$$b_n = \sum_{j=n}^{\infty} \frac{L_{nj}}{L_{jj}} q_j(x), \tag{1.63}$$

where

$$q_j = \frac{1}{k_j} \int_{\tau_1} Q_j(x)\ U_1(x) dx.$$

Hence, all the unknown coefficients b_n and c_n can be determined through equations (1.63) and (1.55), respectively.

1.7.3 Wiener-Hopf method

In Wiener's own words, "*The various types of particles which form light and matter exist in a sort of balance with one another, which changes abruptly when we pass beyond the surface of the star. It is easy to set up the equations for this equilibrium, but it is not easy to find a general method for the solution of these equations" [44].* Thus, the Wiener–Hopf technique was first propounded as a means to solve, for $f(x)$ is an integral equation of the form

$$\int_0^{\infty} K(x-y)\ f(y)\ dy = g(x),\ 0 < x < \infty,$$

where $k(x-y)$ is a known difference kernel, and g(x) is a specified function defined over the half-line $x > 0$. The method proceeds by extending the domain to negative real values of x. Thus, we write

$$\int_0^{\infty} K(x-y) f(y) dy = \begin{cases} g(x),\ 0 < x < \infty, \\ h(x),\ -\infty < x < 0, \end{cases} \tag{1.64}$$

where $h(x)$ is unknown function.

Fourier transformation of equation (1.64) then yields the typical Wiener–Hopf functional equation, given as [45]

$$G_+(s) + H_-(s) + F_+(s)K(s) = 0,$$

where H_- and $F_+(s)$ are half-range Fourier transforms (Section 1.6.1) (defined over $(-\infty, 0)$ and $(0, \infty)$), respectively) of the unknowns $h(x)$ and $f(x)$. By contrast, the quantities $G_+(s)$ (half-range Fourier transform of a function $g(x)$) and $K(s)$ (full-range Fourier transform of the function $K(x)$) are known functions. The product form of the right-hand side of this equation is due to the fact that the original integral operator is of convolution type. The subscripts $+$ $(-)$ indicate that the respective functions are analytic in the upper (lower) half regions of the transformed complex s-plane. The Wiener–Hopf procedure hinges on finding a product factorization for the Fourier-transformed kernel in the form

$$K(s) = K_+(s)/K_-(s).$$

Theorem 1.1. *Cauchy theorem [46]: If $f(\xi)$ is an analytic function, continuous within and on a simple closed curve C and if $f'(\xi)$ exists at each point within C, then*

$$\int_C f(\xi)d\xi = 0. \tag{1.65}$$

Proof. Proof of the theorem can be found in [46]. □

Theorem 1.2. *Cauchy Integral Form: If $f(\xi)$ is an analytic function, continuous within and on a simple closed curve C and if $f'(\xi)$ exists at each point within C and* *let α be any point within C, then*

$$f(\alpha) = \frac{1}{2\pi\iota}\int_C \frac{f(\xi)}{\xi-\alpha}d\xi. \tag{1.66}$$

Proof. Proof of the theorem can be found in [46]. □

Theorem 1.3. *Liouville Theorem: Every bounded entire function is constant.*

Proof. Proof of the theorem can be found in [46]. □

Theorem 1.4. *Extended Liouville Theorem: Let $f(\xi)$ be entire function such that*

$$|f(\xi)| < M|\xi|^p \text{ as } |\xi| \to \infty,$$

then $f(\xi)$ is a polynomial of degree at most $[p]$.

Theorem 1.5. *[47] Let $f(s)$ be an analytic function of $s = \sigma + \iota\tau$, regular in the strip $\tau_- < \tau < \tau_+$ such that $|f(\sigma+\iota\tau)| < |\sigma|^{-p}$; $p > 0$ for $|\sigma| \to \infty$ and if $\tau_- + \epsilon < \tau < \tau_+ - \epsilon$; $\epsilon > 0$, then for $\tau_- < c < \tau < d < \tau_+$,*

$$f(s) = f_+(s) + f_-(s), \tag{1.67}$$

$$f_+(s) = \frac{1}{2\pi\iota}\int_{\infty+\iota c}^{\infty+\iota c} \frac{f(\xi)}{\xi - s}d\xi, \tag{1.68}$$

$$f_-(s) = -\frac{1}{2\pi\iota}\int_{\infty+\iota d}^{\infty+\iota d} \frac{f(\xi)}{\xi - s}d\xi, \tag{1.69}$$

where $f_+(s)$ is regular for $\forall\ \tau > \tau_-$ and $f_-(s)$ is regular for $\tau < \tau_+$.

Proof. Proof of the theorem can be found in [47]. □

Theorem 1.6. *[47] Let $K(s)$ be an analytic function of $s = \sigma + \iota\tau$, regular and non-zero in the strip $\tau_- < \tau < \tau_+$, $K(s) \to 1$ as $\sigma \to \pm\infty$, then*

$$K(s) = K_+(s)K_-(s), \tag{1.70}$$

where $K_+(s)$ and $K_-(s)$ are regular, bounded and non-zero for $\forall\ \tau > \tau_-$ and $\tau < \tau_+$, respectively.

Proof. Let $f(s) = \ln K(s)$ in Theorem 1.5, then

$$\ln K(s) = \frac{1}{2\pi\iota}\int_{\infty+\iota c}^{\infty+\iota c}\frac{\ln K(\xi)}{\xi - s}d\xi - \frac{1}{2\pi\iota}\int_{\infty+\iota d}^{\infty+\iota d}\frac{\ln K(\xi)}{\xi - s}d\xi. \tag{1.71}$$

□

1.8 Thesis organisation

The thesis is organized into five chapters in addition to the present Chapter 1: Introduction, which briefly describes the concepts of fracture mechanics and the definitions. The chapter introduces the topics of FM, different physical parameters, mathematical concepts, and methodologies that have been used in the thesis. Chapter 2 contains a mathematical formulation of the problem with cracks under uniform heat flow. The geometry of the problem includes a central crack of length $2a$, and another crack is present at a distance e and height h from the origin. Singular integral equations with Cauchy kernels have been obtained for temperature and stress fields. The chapter uses the expansion collocation method with Chebyshev polynomials of the first kind to calculate the SIFs at crack tips numerically. Results depict the expressions for SIFs, and graphs depict the variations in mode-I SIFs for varying crack length ratios and strip width. The results reveal the dependency of physical parameters on the lengths of the cracks, their varying distances from each other, and the width of the strip. Chapter 3 addresses the crack problem in an anti-plane coordinate system. Mathematical formulation of the problem in dissimilar orthotropic mediums under mechanical loadings and the corresponding boundary conditions have been depicted. In the chapter, Jacobi polynomials of the first kind have been used to convert the singular integral equation problem into a system of algebraic equations. Jacobi polynomials are the generalization of Chebyshev polynomials and form an orthogonal set with respect to appropriate weight function, which has been discussed in the chapter. The results reveal the plots for SIFs vs. crack lengths and strip width for different particular cases of material selections. A moving semi-infinite crack at the interface of dissimilar strips has been addressed in Chapter 4. The classical Wiener-Hopf method has been used for the complex-valued transformed plane to solve the problem of unknown function in the half-plane. Galilean transformation has been used to convert the problem into a static problem, and parameters like SIF, SMF, and crack energy have been computed. Their graphical representations through two-dimensional and three-dimensional graphs provide a detailed analysis of the results. A particular case has been considered in one of the sections of the chapter to calculate the SMF. The numerical results reveal the physical parameters of stresses by variations in crack and shear wave velocities. Partially insulated cracks in the orthotropic medium under the influence of thermal and mechanical loadings have been studied in Chapter 5. The Schmidt method has been used for numerical computations, and the results reveal the SIFs for mode-I and mode-II, as well as HFIF and crack displacements for various cases. Numerical validations and comparisons have been carried out with previous known results. The expressions have been computed semi-analytically and plotted for different particular cases numerically. The results reveal the dependency among various parameters of crack length, strip width, thermal conductivity, displacements, stress, and displacement. Lastly, Chapter 6 is divided into two sub-sections, which contain the overall conclusion of the thesis in detail and future works. Each chapter's brief conclusion has been presented in the chapter which summarises the whole thesis. Limitations of the study and subsequent future works have been discussed by providing some alternate models.

****